CR-102766

Lockheed

HUNTSVILLE RESEARCH & ENGINEERING CENTER

LOCKHEED MISSILES & SPACE COMPANY

A GROUP DIVISION OF LOCKHEED AIRCRAFT CORPORATION

HUNTSVILLE, ALABAMA

HREC-0154-1
LMSC/HREC D162322

LOCKHEED MISSILES & SPACE COMPANY
HUNTSVILLE RESEARCH & ENGINEERING CENTER
HUNTSVILLE RESEARCH PARK
4800 BRADFORD DRIVE, HUNTSVILLE, ALABAMA

BASE RECIRCULATION FLOW PREDICTION USING A TIME-DEPENDENT FINITE-DIFFERENCE TECHNIQUE

May 1970

Contract NAS8-30154

by

William R. Waldrop

Prepared for National Aeronautics and Space Administration
Marshall Space Flight Center, Alabama

APPROVED:

J. W. Benefield, Supervisor
Propulsion Section

G. D. Reny, Manager
Aeromechanics Dept.

for J. S. Farrior
Resident Manager

FOREWORD

This is the final report of a theoretical investigation of "S-IC Base Radiation and Plume Interaction Reversed Flow Study." This report presents documentation for the base flow analysis effort performed on the study. Documentation for other efforts have been published previously and are not repeated here (NASA CR-61321, "User's Manual for "RAVFAC" - A Radiation View Factor Digital Computer Program," by J. K. Lovin and A. W. Lubkowitz, LMSC/HREC D148620, November 1969). This work was performed by Lockheed Missiles & Space Company, Huntsville Research & Engineering Center, for the Aero-Astrodynamics Laboratory of the National Aeronautics and Space Administration, George C. Marshall Space Flight Center, under Contract NAS8-30154.

Technical monitors for this contract were Mr. H. B. Wilson, Jr., Mr. R. F. Elkin, and Mr. E. B. Brewer of the Thermal Environment Branch, Aero-Astrodynamics Laboratory, MSFC.

SUMMARY

Problems associated with computing the three-dimensional base recirculation flow of a perfect gas from multiple-clustered nozzles are discussed. A Lax-Wendroff time-dependent, finite-difference numerical scheme is presented as the most desirable technique for computing this flow field. Results of a preliminary investigation indicated that including viscous terms in this analysis was impractical because of the number of grid points required for accurate resolution within strong viscous regions. However, inclusion of viscous terms was deemed unnecessary for computing the overall flow field. A cylindrical coordinate system with the axis at the center of the nozzle cluster simplified the specification of some boundary conditions, but extrapolation was required to specify conditions downstream of the nozzles and around the exterior of the nozzle wall. Stretching transformations are presented which concentrate grid points in the regions of the plume interaction. A possible modification to the numerical scheme which would permit using a steady form of the energy equation and, hence, reduce computer storage requirements is discussed. Stability of the numerical technique used in this study is also analyzed. Two techniques are presented for controlling the time step to ensure stability during the computation. The first technique monitors the total change between time steps of all dependent variables over the entire flow field and controls the time step to ensure that this total change decreases. The second technique prevents using a time step large enough to cause a provisional value of density to go negative at any grid point. Conclusions resulting from this analysis and recommendations for future investigations are presented.

CONTENTS

NOMENCLATURE

a	centrifugal force vector for cylindrical coordinate system (Eq. (2.10e))
B	$\partial \tau / \partial \theta$
c	speed of sound
c_v	specific heat at constant volume
E	total energy
e	internal energy per unit mass
f	vector used to compute changes in x direction (Eq. (2.10b))
g	vector used to compute changes in r direction (Eq. (2.10c))
$\bar{g}$	quantity used to monitor change of dependent variables (Eq. (2.28)
h	vector used to compute changes in θ direction (Eq. (2.10d))
K_r	stretching constant in r direction
K_τ	stretching constant in τ direction
n	time step
NCN	number of concentric nozzles
p	pressure
q	velocity vector
R	axisymmetric radial distance
$\mathcal{R}$	gas constant
r	radial distance (Fig. 2)
$\tilde{r}$	incremental parameter for stretching in r direction
T	temperature

NOMENCLATURE (Continued)

t	time
U	axisymmetric velocity component in X direction (Fig. 4)
u	velocity component in x direction
V	axisymmetric velocity component in R direction (Fig. 4)
v	velocity component in r direction
w	velocity component in θ direction
X	axisymmetric longitudinal distance aft of nozzle exit plane
x	longitudinal distance aft of nozzle exit plane
x_o	negative longitudinal distance from nozzle exit plane to heat shield
y_o	radial distance from nozzle centerline to centerline of cluster

Greek

β	tangency angle of nozzle exterior wall in r-θ plane (Fig. 3)
γ	ratio of specific heats
Δ	step size
δ	spatial step size
θ	angular direction
θ_o	angle defining reflection plane between nozzles (Fig. 2)
ρ	density
τ	normalized parameter in θ direction
$\tilde{\tau}$	incremental parameter for stretching in θ direction
ϕ	angle between axisymmetric velocity vector and nozzle centerline (Fig. 4)
ω	vector form of dependent variables (Eq. (2.10a))

NOMENCLATURE (Continued)

Subscripts

w	condition at exterior of nozzle wall
t	total reference condition
i, j, k	indices for grid points in x, r, θ directions, respectively
0	value at previous time
1	value at current time

Section 1
INTRODUCTION

Interaction of exhaust plumes from multiple rocket nozzle configurations, as shown in the example configuration of Fig. 1, creates a complex three-dimensional network of shock waves. If the impingement angle is large, which is usually the case of highly underexpanded plumes, these shock waves may detach from a plane of symmetry existing between the plumes. This will allow extremely hot gases to recirculate around the heat shield and the exterior of the rocket nozzle; thus, heat transfer to these components could be significantly increased. Although base recirculation is a well-recognized problem of launch and space vehicles, the three-dimensionality of the flow has prevented thorough analyses. Experimental investigations (Ref. 1) have yielded some insight into the mechanism of these flows, but applicability of these data are very limited. The purpose of this study is to develop a theoretical technique which would provide the required flexibility for investigating the base recirculation flow field of multi-nozzle configurations.

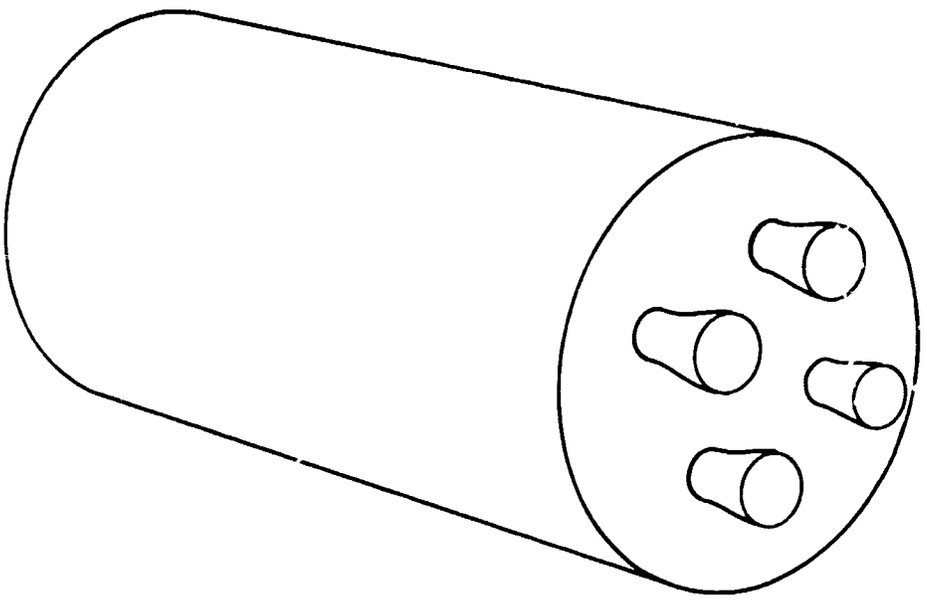

Fig. 1 — Example of Four Nozzle Configurations

Section 2
TECHNICAL DISCUSSION

2.1 SELECTION OF TECHNIQUE FOR SOLUTION OF FLOWFIELD EQUATIONS

Of all the techniques used to solve fluid mechanic problems, closed-form analytical solutions are obviously the most desirable. Unfortunately, the conservation equations of fluid motion contain nonlinear partial differential equations. Closed-form solutions to these equations require that they be linearized either by transformations or by simplifying assumptions. The complexity of the equations describing the three-dimensional base recirculation flow field, which contains shock waves and resulting regions of subsonic and supersonic flow, precludes either transformations or approximations that are valid over the entire field.

Numerical solutions of the conservation equations of this recirculation flow present the only alternative. Spatial marching techniques, such as the method of characteristics or the steady-state form of the Lax-Wendroff technique, have been used with apparent success for plume interaction problems which are limited to oblique shock waves at the interacting reflection planes (Refs. 2 and 3). Such initial-value techniques are restricted to regions of hyperbolic flow; hence, they are entirely inadequate for analysis of flow containing detached shocks with regions in which the equations are elliptic in nature.

Two classes of numerical techniques which appear most attractive for the solution of this type of problem are asymptotic time-dependent unsteady techniques and relaxation techniques. Both classes involve solving finite-difference approximations to the Eulerian equations of motion. The time-dependent techniques use the principle that the unsteady Eulerian equations

are hyperbolic in nature; thus, marching forward in time is possible. If the time step is appropriately small such that the numerical scheme is stable, the unsteady flow will asymptotically approach the steady-state solution.

One of the few formalized relaxation techniques for fluid mechanics applications was recently presented by Prozan (Ref. 4). His technique, known as the Error Minimization Technique (EMT), uses the steady Eulerian form of the conservation equations, but these equations are set equal to an error term for each equation at each grid point. Because an initial flow field with imposed boundary conditions does not satisfy these conservation equations, this error term is non-zero. A positive definite merit function of the error term is defined, and the merit function is decreased through descent techniques. As this merit function asymptotically approaches zero, the flow variables approach their correct steady-state values. Comparisons with time-dependent techniques indicate that the EMT is equally as accurate and requires comparable computation time as the unsteady techniques require for convergence.

The feasibility of including viscous terms in an analysis of this type was considered. Both the unsteady and relaxation methods are capable of solutions involving these terms. However, a preliminary investigation indicates that a fine mesh grid system was required to obtain resolution in regions where the viscous stresses dominate. When considering the staggering number of grid points required to define the inviscid three-dimensional flow field, it was concluded that the inclusion of enough additional grid points to yield meaningful results of a viscous flow field of this type was impractical. It was further concluded that the exclusion of viscous forces from the analysis would not significantly affect the characteristics of the overall flow field, although the possibility of rationalization is conceded.

Infinitesimally thin shock waves of various strength will obviously exist throughout the flow field under consideration. State-of-the-art, finite-difference techniques are not able to correctly isolate the location of shocks

between grid points, treat them as discrete discontinuities, and apply shock jump conditions. An attempt to improve the state of the art to accomplish this was unsuccessful. An alternative approach was to introduce artificial viscosity into the equations. This may be done explicitly as presented by von Neumann and Richtmyer (Ref. 5) or implicitly as done by Lax and Wendroff (Ref. 6). Either approach introduces dissipation terms which become large in regions of high compression. As a result, shock waves occur over several grid points. The effect of this smearing can often be reduced by using a finer grid mesh.

Presumably, because of the similarity of the formulation of the equations, shock smearing versions could exist for either EMT or unsteady techniques. However, several versions of the unsteady techniques have proven quite capable of computing flow fields with shock waves; whereas a shock smearing version of EMT would require additional development. For this reason, a recent version of the finite-difference, two-step Lax-Wendroff unsteady technique is presented in Section 2.4 of this report for solving the three-dimensional base recirculation flow field. This technique has been coded in FORTRAN V for use on the Univac 1108 digital computer. The following sections of this report describe the application of this technique to the base recirculation problem, as well as a derivation of the finite-difference scheme.

2.2 GEOMETRY CONSIDERATIONS

The computation technique has much versatility in respect to geometry considerations. Flow from any number of nozzles may be computed so long as they are positioned concentrically about a central point. Figure 2 presents an example of a four-nozzle configuration. The end view reveals eight reflection planes for this configuration. Because of this symmetry, it is necessary to investigate only one-eighth of the entire flow field for this configuration. All distances are nondimensionalized by the exit diameter of the nozzle. The effect of nozzle separation distance relative to the exit diameter

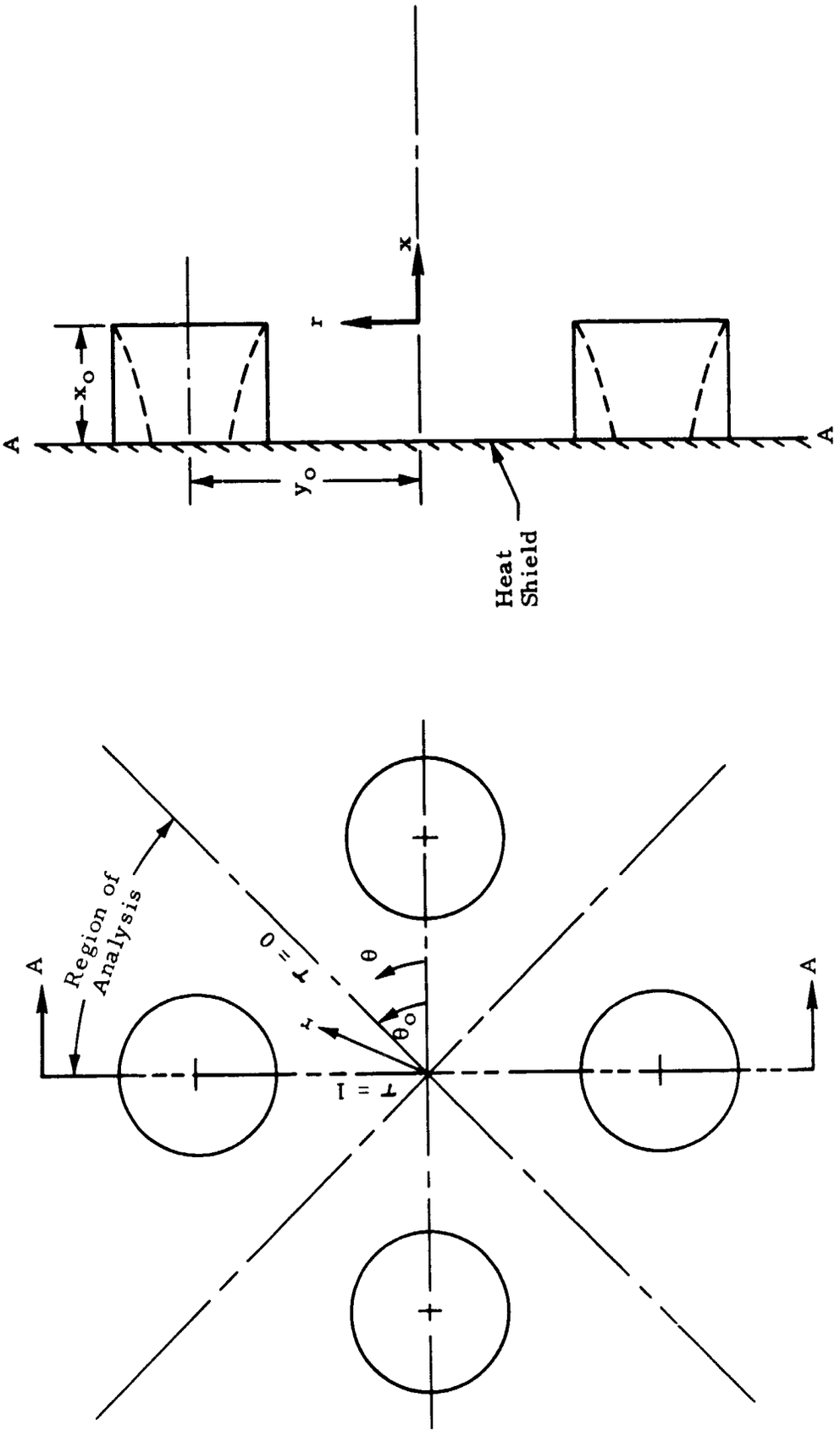

Fig. 2 - Three-Dimensional Cylindrical Coordinate System of a Four-Nozzle Configuration

may be studied by choosing various values of y_o. The heat shield location is designated x_o, where $x_o \leq 0$.

2.2.1 Coordinate System

The choice of a cylindrical coordinate system is natural when considering the region of analysis. The angle from the reference line to the first plane of symmetry θ_o is computed from the geometry by

$$\theta_o = \frac{\pi}{2} - \frac{\pi}{NCN} \tag{2.1}$$

where NCN is the number of concentric nozzles. For convenience of notation, a normalized parameter τ is defined as

$$\tau \equiv \frac{\theta - \theta_o}{\frac{\pi}{2} - \theta_o} \quad ; \tag{2.2}$$

thus, $\tau = 0$ and 1 represents the two reflection planes.

2.2.2 Exterior Nozzle Wall Equations

The exterior wall of the nozzle is represented as a cylinder as shown in Fig. 2. For this offset cylindrical coordinate system, the equation for this nozzle exterior wall is

$$\sin\theta_w = \frac{r_w^2 + y_o^2 - \frac{1}{4}}{2 y_o r_w} \tag{2.3}$$

if $(r - \frac{1}{2}) \leq y_o \leq (r + \frac{1}{2})$ and $x \leq 0$.

By defining β_w as the angle between the tangent of the exterior wall and the horizontal in the $r - \theta$ plane (Fig. 3), then

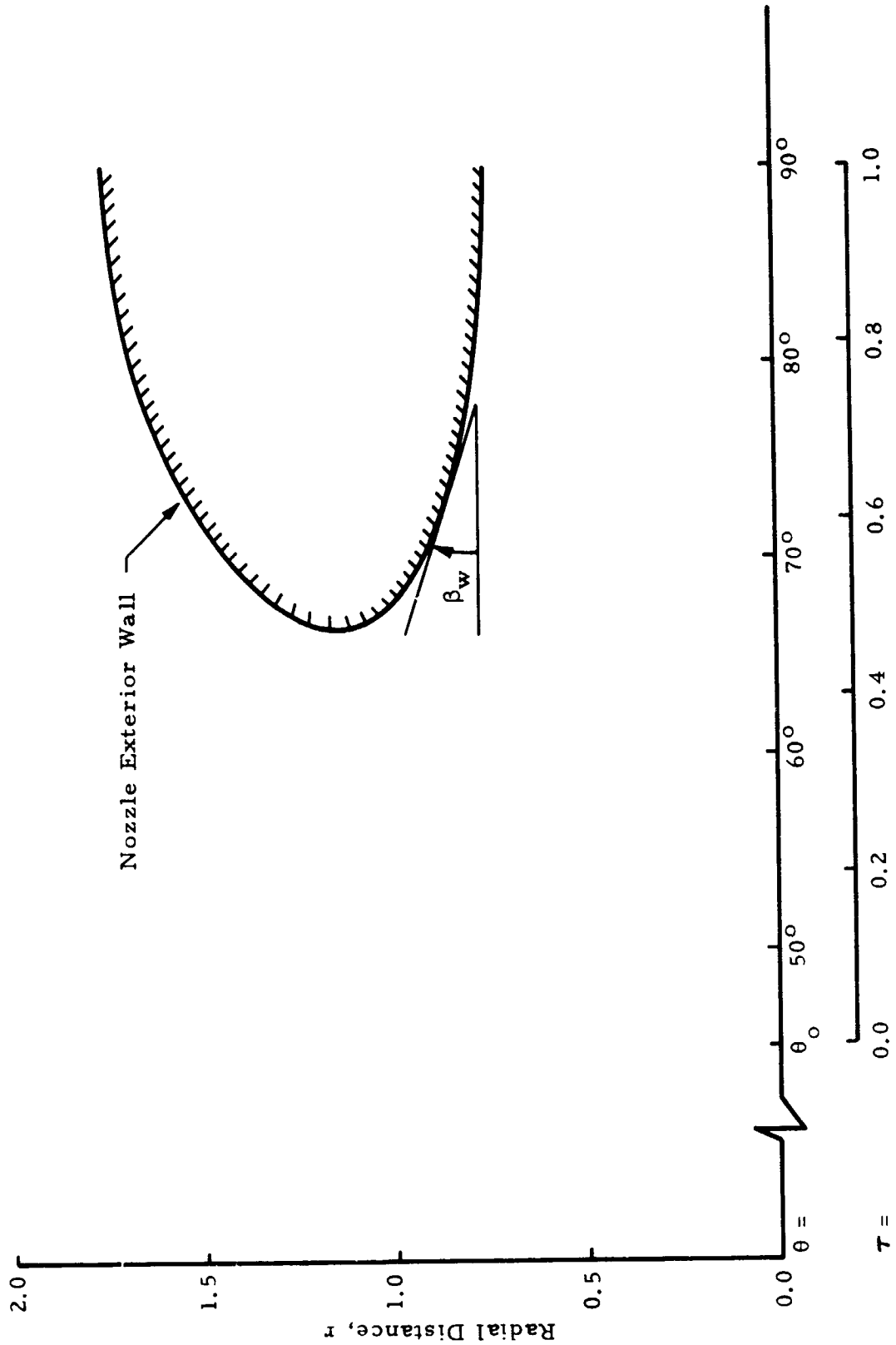

Fig. 3 - Nozzle Exterior Wall in Unstretched r-θ Plane (Four-Nozzle Configuration)

$$\tan\beta_w \equiv \frac{d\,r_w}{d\,\theta_w}$$

$$= y_o \cos\theta_w \left[1 - \frac{y_o \sin\theta_w}{\pm\sqrt{\frac{1}{4} - y_o^2 \cos^2\theta_w}} \right] . \qquad (2.4)$$

This angle will be used to specify tangential flow about the nozzle exterior wall.

2.2.3 Stretching Transformations

By visualizing flow for the nozzles in Fig. 2, it may be seen that plumes will first interact and cause shock waves along $\tau = 0$. Slightly farther downstream all four plumes will intersect at $r = 0$ causing a complex flow pattern to occur inside a diamond-shape shock wave for the four-nozzle configuration. For these reasons, increased emphasis should be placed on defining the region near $\tau = 0$ and $r = 0$. The following stretching transformation is suggested to provide a fine mesh grid near $\tau = 0$:

$$\tau \equiv \tilde{\tau} - K_\tau \sin(\pi\tilde{\tau}) \qquad (2.5)$$

where

K_τ = arbitrary constant less than $\frac{1}{\pi}$

$\tilde{\tau}$ = parameter varied from 0 to 1 by even increments

A similar stretching transformation in the r direction is suggested as

$$r = \tan(K_r \tilde{r}) \qquad (2.6)$$

where

K_r = arbitrary constant

$\tilde{r}$ = parameter which may be varied from 0 to $\pi/2K_r$ by even increments

2.2.4 Number of Grid Points

Approximately 50 grid points in the x direction, 25 in the r direction, and 23 in the τ direction are estimated to be the minimum number of grid points required for adequate resolution of a typical problem for the geometry shown in Fig. 2. This total comes to nearly 30,000 grid points. It will be shown in Section 2.4 that 10 dependent variables must be stored at each grid point. This requires storing 300,000 variables which greatly exceeds the core storage of any digital computer available locally. A rapid access drum storage routine of the Univac 1108 digital computer provides an alternative to core storage. This routine known as NTRAN has been modified to relinquish control of the machine while performing the time-consuming chore of repositioning the drum to a desired location. Combining a restart capability with this routine would be desirable to prevent loss of converging flowfield parameters through machine error.

2.3 BASIC DIFFERENTIAL EQUATIONS

The unsteady conservation of mass and energy equations, the three unsteady Euler equations, and the perfect gas relation give six equations in six unknowns. These unknowns are the three velocity vectors (u, v, w), pressure (p), total energy (E), and density (ρ). The pressure may immediately be eliminated from these equations by considering the perfect gas relation

$$\hat{p} = \hat{\rho}\hat{R}\hat{T}$$

$$= (\gamma - 1)\hat{\rho}\hat{C}_v\hat{T}$$

$$= (\gamma - 1)\hat{\rho}\hat{e}$$

Nondimensionalizing* by the reference total density $\hat{\rho}_t$ and speed of sound $\hat{c}_t$ gives

*Note: Quantities with ($\hat{}$) denote dimensional variables.

$$p = (\gamma - 1)\,\rho e$$

Using the definition of the total energy as the sum of the internal and kinetic energies

$$E \equiv \rho\left[e + \frac{1}{2} q^2\right] \tag{2.7}$$

where

$$q^2 \equiv u^2 + v^2 + w^2$$

yield the pressure as

$$p = (\gamma - 1)\left[E - \frac{\rho q^2}{2}\right]. \tag{2.8}$$

This expression is used to eliminate pressure from the Euler equations and the conservation of energy equation. This leaves the following set of five equations and five unknowns shown in vector notation as

$$\frac{\partial \omega}{\partial t} = -\left[\frac{\partial f}{\partial x} + \frac{\partial g}{\partial r} + \frac{1}{r}\frac{\partial h}{\partial \theta} + \frac{a}{r}\right] \tag{2.9}$$

where

$$\omega = \begin{pmatrix} \rho \\ \rho u \\ \rho v \\ \rho w \\ E \end{pmatrix} \tag{2.10a}$$

$$f = \begin{pmatrix} (\rho u) \\ (\gamma - 1)E - \left(\frac{\gamma - 3}{2}\right)\left(\frac{1}{\rho}\right)(\rho u)^2 - \left(\frac{\gamma - 1}{2}\right)\left(\frac{1}{\rho}\right)\left[(\rho v)^2 + (\rho w)^2\right] \\ (\rho u)(\rho v)\left(\frac{1}{\rho}\right) \\ (\rho u)(\rho w)\left(\frac{1}{\rho}\right) \\ \frac{\gamma E}{\rho}(\rho u) - \left(\frac{\gamma - 1}{2}\right)\left(\frac{1}{\rho^2}\right)(\rho u)\left[(\rho u)^2 + (\rho v)^2 + (\rho w)^2\right] \end{pmatrix} \quad (2.10b)$$

$$g = \begin{pmatrix} (\rho v) \\ (\rho u)(\rho v)\left(\frac{1}{\rho}\right) \\ (\gamma - 1)E - \left(\frac{\gamma - 3}{2}\right)\left(\frac{1}{\rho}\right)(\rho v)^2 - \left(\frac{\gamma - 1}{2}\right)\left(\frac{1}{\rho}\right)\left[(\rho u)^2 + (\rho w)^2\right] \\ (\rho v)(\rho w)\left(\frac{1}{\rho}\right) \\ \frac{\gamma E}{\rho}(\rho v) - \left(\frac{\gamma - 1}{2}\right)\left(\frac{1}{\rho^2}\right)(\rho v)\left[(\rho u)^2 + (\rho v)^2 + (\rho w)^2\right] \end{pmatrix} \quad (2.10c)$$

$$h = \begin{pmatrix} (\rho w) \\ (\rho u)(\rho w)\left(\frac{1}{\rho}\right) \\ (\rho v)(\rho w)\left(\frac{1}{\rho}\right) \\ (\gamma - 1)E - \left(\frac{\gamma - 3}{2}\right)\left(\frac{1}{\rho}\right)(\rho w)^2 - \left(\frac{\gamma - 1}{2}\right)\left(\frac{1}{\rho}\right)\left[(\rho u)^2 + (\rho v)^2\right] \\ \frac{\gamma E}{\rho}(\rho w) - \left(\frac{\gamma - 1}{2}\right)\left(\frac{1}{\rho^2}\right)(\rho w)\left[(\rho u)^2 + (\rho v)^2 + (\rho w)^2\right] \end{pmatrix} \quad (2.10d)$$

$$a = \begin{pmatrix} (\rho v) \\ (\rho u)\ (\rho v)\left(\frac{1}{\rho}\right) \\ \left(\frac{1}{\rho}\right)\left[(\rho v)^2 - (\rho w)^2\right] \\ \left(\frac{2}{\rho}\right)(\rho v)\ (\rho w) \\ \left(\frac{1}{\rho}\right)(\rho v)\left\{\gamma E - \left(\frac{\gamma - 1}{2}\right)\left(\frac{1}{\rho}\right)\left[(\rho u)^2 + (\rho v)^2 + (\rho w)^2\right]\right\} \end{pmatrix} \qquad (2.10e)$$

These equations, expressed in conservative form, treat (ρu), (ρv), and (ρw) as dependent variables instead of u, v, w.

An alternate form of these equations in which E may be expressed as a function of the remaining four dependent variables is proposed. Combining the adiabatic, perfect gas relation,

$$\frac{\hat{T}}{\hat{T}_t} = 1 - \left(\frac{\gamma - 1}{2}\right)\frac{\hat{q}^2}{\hat{a}_t^2}$$

$$= 1 - \left(\frac{\gamma - 1}{2}\right) q^2$$

with the specific internal energy relation,

$$\hat{e} = \hat{c}_v \hat{T}$$

$$= \frac{\hat{R}}{(\gamma - 1)} \hat{T}$$

and the thermally perfect expression of the speed of sound,

$$\hat{c}_t^2 = \gamma \hat{R}_t \hat{T}_t$$

gives

$$e = \frac{1}{\gamma}\left(\frac{1}{\gamma - 1} - \frac{1}{2} q^2\right) .$$

The total energy E may then be explicitly expressed as a function of the other four dependent variables by

$$E = \frac{\rho}{\gamma}\left\{\frac{1}{\gamma - 1} + \left(\frac{\gamma - 1}{2}\right) q^2\right\}$$

$$= \frac{\rho}{\gamma}\left\{\frac{1}{\gamma - 1} + \left(\frac{\gamma - 1}{2}\right) \frac{1}{\rho^2}\left[(\rho u)^2 + (\rho v)^2 + (\rho w)^2\right]\right\} . \qquad (2.11)$$

Equation (2.11), which is not in differential form, can be used to decrease the computer storage variables by 20%. Preliminary investigations on simplified flow fields indicate that convergence time is not significantly altered by using Eq. (2.11) to solve for the energy directly. The computer program does not include this option because of the preliminary nature of these results.

2.4 SOLUTION OF UNSTEADY FINITE-DIFFERENCE EQUATIONS

The solution to Eq. (2.9) begins by expanding the vector Eq. (2.10a) in the Taylor series

$$\omega^{t_1}_{i,j,k} = \omega^{t_0}_{i,j,k} + \left(\frac{\partial \omega}{\partial t}\right)^{t_0}_{i,j,k} \Delta t + C(\Delta t)^2 \qquad (2.12)$$

where superscript t refer to time and subscripts i, j, k refer to grid point numbers in the x, r, θ directions Direct substitution of Eq. (2.9) into Eq. (2.12) gives

$$\omega^{t_1}_{i,j,k} = \omega^{t_0}_{i,j,k} - \left[\left(\frac{\partial f}{\partial x}\right)^{t_0}_{i,j,k} + \left(\frac{\partial g}{\partial r}\right)^{t_0}_{i,j,k} + \left(\frac{1}{r}\,\frac{\partial h}{\partial \theta}\right)^{t_0}_{i,j,k} + \left(\frac{a}{r}\right)^{t_0}_{i,j,k}\right]\Delta t + 0(\Delta t)^2 . \qquad (2.13)$$

Any finite-difference analogy to Eq. (2.13) is unconditionally unstable; however, this equation can be modified into a form which is conditionally stable. One popular technique is to retain higher order terms, but this involves the complicated and computer time-consuming process of expressing $\partial^2\omega/\partial t^2$ as a function of $\partial^2 f/\partial x^2$, $\partial^2 f/\partial x\,\partial r$, etc.

A preferred method of stabilizing Eq. (2.13) is by using a two-step process. This process, known as the two-step Lax-Wendroff technique, computes provisional values of ω in the first step which are then averaged with previous values in a second stable step. A three-dimensional, cylindrical coordinate adaptation of a two-step version recently presented by MacCormack (Ref. 7) is suggested for the solution of the base recirculation flow equations. This technique was chosen because it is easy to compute and has second-order accuracy.

Consider the one-dimensional form of Eq. (2.13),

$$\omega_i^{t_1} = \omega_i^{t_0} - \left(\frac{\partial f}{\partial x}\right)_i^{t_o} \Delta t + 0(\Delta t)^2 . \qquad (2.14)$$

The central difference analogy of the partial derivative of Eq. (2.14) may be expressed as

$$\left(\frac{\partial f}{\partial x}\right)_i \approx \frac{f_{i+1} - f_i}{2\Delta x} + \frac{f_i - f_{i-1}}{2\Delta x} + 0(\Delta x)^2 . \qquad (2.15)$$

The first step of the technique which computes provisional values, steps forward in time $2\Delta t$ and uses the forward portion of Eq. (2.15) or

$$\omega_i^{\bar{t}_1} = \omega_i^{t_0} - \left(f_{i+1}^{t_0} - f_i^{t_0}\right) \frac{\Delta t}{\Delta x} . \qquad (2.16)$$

The second and stabilizing step of the process provides second-order accuracy by using the backward portion of Eq. (2.15). This step marches forward in time

Δt from t_0 and averages provisional and original values of ω by

$$\omega_i^{t_1} = \frac{\omega_i^{t_0} + \omega_i^{\bar{t}_1}}{2} - \left(f_i^{\bar{t}_1} - f_{i-1}^{\bar{t}_1}\right) \frac{\Delta t}{2\Delta x}$$

$$= \omega_i^{t_0} - \left(f_{i+1}^{t_0} - f_i^{t_0} + f_i^{\bar{t}_1} - f_{i-1}^{\bar{t}_1}\right) \frac{\Delta t}{2\Delta x} + 0(\Delta t)^2 + 0(\Delta x)^2. \quad (2.17)$$

A three-d. nensional version of Eqs. (2.16) and (2.17) is presented below:

First Step:

$$\omega_{i,j,k}^{\overline{n+1}} = \omega_{i,j,k}^{n} - \frac{\Delta t}{\delta}\left\{\left(f_{i+1,j,k}^{n} - f_{i,j,k}^{n} + \left(g_{i,j+1,k}^{n} - g_{i,j,k}^{n}\right)\right.\right.$$

$$\left.\left. + \frac{1}{r}\left[\left(h_{i,j,k+1}^{n} + h_{i,j,k}^{n}\right)B + (\delta)\left(a_{i,j,k}^{n}\right)\right]\right\} \quad (2.18)$$

Second Step:

$$\omega_{i,j,k}^{n+1} = \frac{1}{2}\left\{\omega_{i,j,k}^{n} + \omega_{i,j,k}^{\overline{n+1}} - \frac{\Delta t}{\delta}\left[\left(f_{i,j,k}^{\overline{n+1}} - f_{i-1,j,k}^{\overline{i+1}}\right) + \left(g_{i,j,k}^{\overline{n+1}} - g_{i,j-1,k}^{\overline{n+1}}\right)\right.\right.$$

$$\left.\left. + \frac{B}{r}\left(h_{i,j,k}^{\overline{n+1}} - h_{i,j,k-1}^{\overline{n+1}}\right)\right] - \frac{\Delta t}{r}\left(a_{i,j,k}^{\overline{n+1}}\right)\right\} \quad (2.19)$$

where

n = superscript used to increment t by $t = (n+1)\,\Delta t$

i, j, k = subscripts referring to grid points in the x, r, τ directions, respectively

$\delta = \Delta x = \Delta r = \Delta\tau$

$B = \frac{\partial \tau}{\partial \theta} = \frac{NCN}{\pi}$.

As suggested by MacCormack, increased stability (larger permissible values of Δt) might be obtained by a cyclic procedure using the forward and backward portions of Eq. (2.15) in the first and second step. Following this suggestion, Eq. (2.13), which consists of three separate partial derivatives, was approximated by eight (i.e., 2^3) combinations of forward and backward finite difference equations. Equations (2.18) and (2.19) represent the first of these eight combinations. Programming these eight schemes was simplified by using a variable indices technique suggested by E. B. Brewer, NASA Technical Monitor.

2.5 BOUNDARY CONDITIONS

The choice of a cylindrical coordinate system (Fig. 2) simplified the specification of boundary conditions. Along the planes $\tau = 0, 1$, reflection principles can be applied with no qualification. Axial symmetry provides the boundary condition at $r = 0$. Because of the singularity of the equations at $r = 0$, the grid was chosen such that this line was straddled. Downstream boundary conditions for maximum values of x were obtained by linear extrapolation. Flow in this region is supersonic; therefore, this approximation appears warranted. Similarly, conditions at maximum values of r were obtained by linear extrapolation. These grid points of r which lie within the plume are again in a supersonic flow regime. It is anticipated that others (i.e., $x < 0$) will have a negligible effect on the plume interaction region.

Conditions along the heat shield are also easy to specify. As pointed out by Moretti (Ref. 8), applying reflection techniques at solid boundaries might constitute improperly forcing to zero certain derivatives in the direction normal to the wall. This could bias the solution. However, it would be possible to substitute a mirror image flow field behind the flat surface of the heat shield without altering the flow. Thus, reflection principles along the heat shield are applicable and were used.

Specifying boundary conditions to ensure that flow about the exterior wall of the nozzle is tangential is more difficult. Figure 3, which shows

the exterior of the nozzle in the r - θ plane, reveals that grid points will not lie on the surface of this wall. From geometry considerations specified in Eq. (2.3), three simple tests will reveal if a grid point lies inside of the nozzle plane. Interior grid points adjacent to the wall may then be used to specify boundary conditions at the wall. An extrapolation in the τ (i.e., θ) direction using values of ρ, ρu, and E at neighboring exterior points provide values of ρ, ρu, and E at the wall and interior adjacent points. Rearranging Eq. (2.11) to solve for q^2 gives a wall value of

$$q_w^2 = \frac{2\gamma}{\gamma - 1}\left[\frac{E_w}{\rho_w} - \frac{1}{\gamma(\gamma - 1)}\right] . \tag{2.20}$$

Multiplying the definition

$$q^2 \equiv u^2 + v^2 + w^2$$

by ρ_w^2 yields

$$(\rho_w q_w)^2 = (\rho u)_w^2 + \rho_w^2 (v_w^2 + w_w^2)$$

or which may be rearranged as

$$\rho_w^2 (v_w^2 + w_w^2) = (\rho_w q_w)^2 - (\rho u)_w^2 .$$

Applying the wall tangency condition gives

$$(\rho v)_w = \left[\sqrt{(\rho_w q_w)^2 - (\rho u)_w^2}\right] \sin \beta_w \tag{2.21}$$

and

$$(\rho w)_w = \left[\sqrt{(\rho_w q_w)^2 - (\rho u)_w^2}\right] \cos \beta_w \tag{2.22}$$

where β_w may be computed from Eq. (2.4).

Boundary values of ρv and ρw at adjacent interior grid points are then obtained by extrapolating in the τ direction using values of ρv and ρw at exterior grid points and those computed at the wall by the tangency condition. Admittedly, this technique involves approximations and assumptions, but it is felt that more sophistication is unwarranted when considering computation time.

Conditions at the nozzle exit are input as initial conditions and not allowed to vary. Grid points at this exit may also be located by using Eq. (2.3).

2.6 INITIAL CONDITIONS

It is desirable to input as initial conditions the best possible values of the dependent variables at each grid point throughout the field. This should significantly decrease the computation time required for convergence to the steady-state solution. For this reason, provisions were made in the computer program for inputting results of a method-of-characteristics (MOC) solution of a single-nozzle configuration.

An interpolation routine is used to determine flowfield parameters at grid points which will not coincide with the axisymmetric characteristic grid points. Figure 4 illustrates the relation between the geometry of the axisymmetric flow of the nozzle and the coordinate system used in this analysis. The calculation of ρ and ρu are obtained directly from the interpolation routine which gives q, ρ, and ϕ at any specified point. The energy E may then be computed from Eq. (2.11).

The two remaining flow variables, ρv and ρw, must be computed from geometry considerations. At a given grid point, values of r and θ are known, and the axisymmetric radial distance may be computed by

$$R = \sqrt{r^2 - 2ry_o \sin\theta + y_o^2} \quad . \tag{2.23}$$

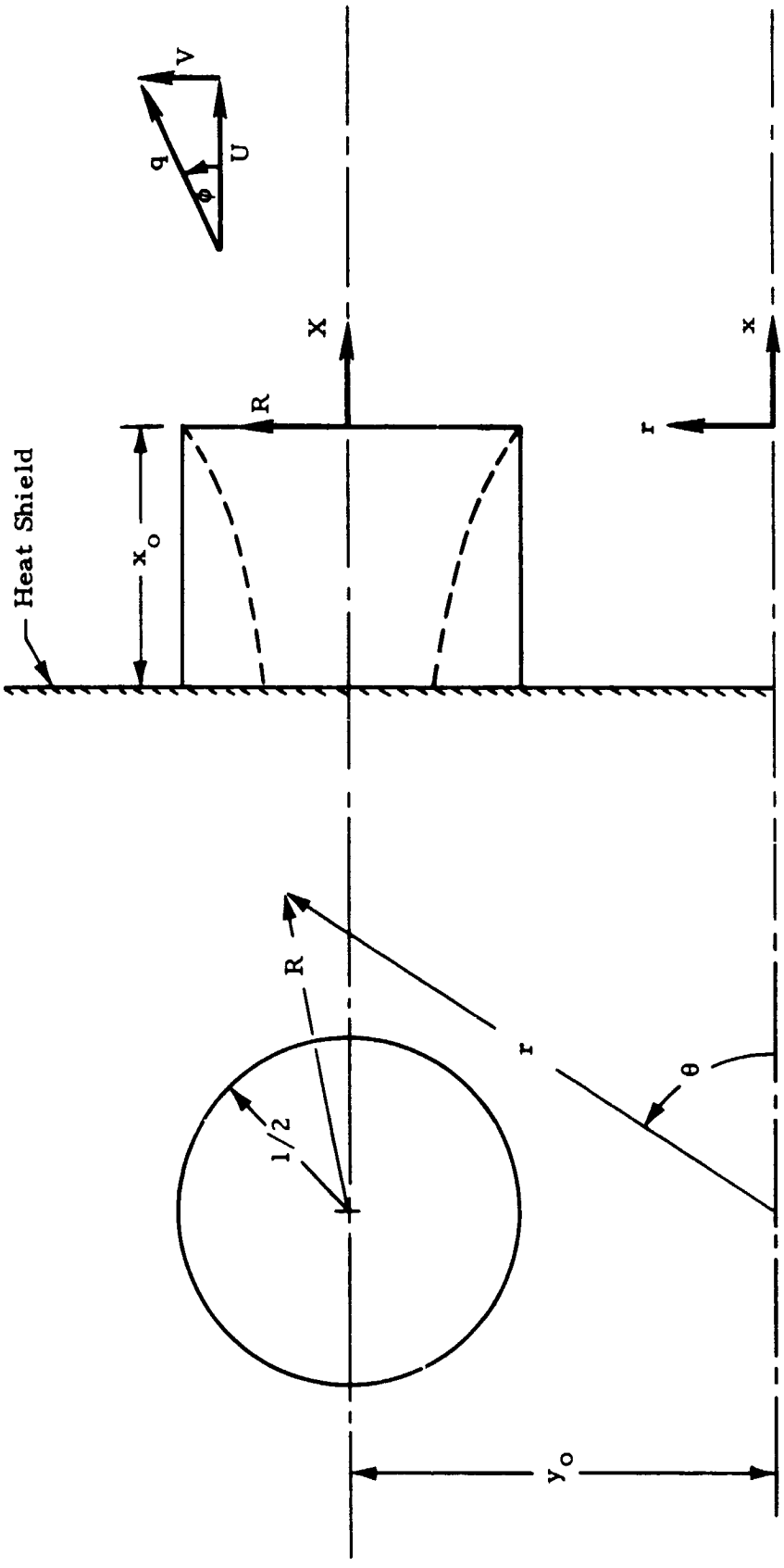

Fig. 4 - Relationship Between Axisymmetric and Three-Dimensional Cylindrical Coordinate Systems

The axisymmetric radial velocity at that point is given by

$$V = q \sin\phi \quad . \tag{2.24}$$

Using Eqs. (2.23) and (2.24) and the fact that the flow is axisymmetric give

$$\rho v = \frac{(r - y_o \sin\theta)\, \rho V}{R} \tag{2.25}$$

and

$$\rho w = - \frac{y_o}{R} \rho V \cos\theta \quad . \tag{2.26}$$

For grid points lying outside of the axisymmetric plume, velocity components are set equal to zero and ambient conditions are prescribed for ρ and E.

Boundary conditions along the $\tau = 0$ plane and the $r = 0$ line are the only ones not identically satisfied. The reflection plane $\tau = 0$ is the plane of impingement of the two plumes; hence, care must be taken in specifying initial conditions along this plane which will not cause an initial instability. Following a suggestion by D'Attorre (Ref. 9), density and energy will be left as computed by the MOC program. Likewise, the computed parameter ρu will be left unchanged, but ρw will be set to zero with the calculated value of ρw added to the calculated value of ρu at that point.

Reflection principles are used to specify boundary values of parameters across the $\tau = 0$ plane, and axial symmetry is used across the $r = 0$ line.

2.7 STABILITY

A stable time-dependent technique is one which begins with an initial unsteady flow field and modifies flow variables so that they asymptotically converge to steady-state values. The maximum possible time step is given by

$$\frac{\Delta t}{\delta}\left(|q| + c\right) \leq 1 \tag{2.27}$$

which is the well-known Courant-Friedricks-Lewy (CFL) condition. For this analysis, it should be noted that the appropriate δ to be considered for Eq. (2.27) is the smallest value of Δx, Δr, or $\Delta \theta$, regardless of stretching transformations used.

A more restrictive stability condition for unsteady techniques is presented by Von Neumann. Unfortunately, this condition can only be applied to linearized equations, but linearization of the flow equations over the entire flow field is impossible because of the presence of shock waves and boundaries. It was, therefore, concluded that any attempt to predict a priori a stable time step, and claim that this time step should apply over the entire field throughout the analysis, would be unrealistic. Alternative approaches for measuring stability were, therefore, sought.

One alternative approach is to use a technique similar to that used by Prozan in the EMT. By defining

$$\bar{g} = \sqrt{\sum_{i,j,k}\left[\left(\rho^{n}_{i,j,k} - \rho^{n-1}_{i,j,k}\right) + \left(\rho u^{n}_{i,j,k} - \rho u^{n-1}_{i,j,k}\right)^2 + \ldots + \left(E^{n}_{i,j,k} - E^{n-1}_{i,j,k}\right)^2\right]} \tag{2.28}$$

it is possible to monitor the total change of flow variables from one time step to the next. If it is appropriate to assume that the initial flow field, with boundary conditions applied, is more different from the steady-state flow than at any time during the convergence process, then $\bar{g}$ should be largest initially. By monitoring $\bar{g}$ and controlling the time step, it is possible to force $\bar{g}$ to monotonically decrease toward the asymptotic value of zero. Comparisons of $\bar{g}$ to a previous value should be made only after a complete cycle of the difference schemes discussed in Section 2.4 because some combinations of forward and backward differences are more stable and allow less change than others. It is possible that this technique of controlling the time step by monitoring $\bar{g}$ could result in neutral stability

(i.e., instability prevented, but the solution does not converge). Results obtained by this technique should be analyzed to ensure that the solution represents a reasonable steady-state flow field.

A second approach to monitoring stability is the antimatter (negative density) method. An initial time step of slightly less than that given by the CFL condition (Eq. 2.27) is assumed. Throughout the computer calculations, the provisional value of density calculated at each grid point during the first step is monitored. If this density should become negative, the time step is decreased and new provisional values are computed over the entire flow field. The basis for this procedure is the fact that all variables change more during the first step than during the second; hence, stability of variables computed by the second step might be maintained by rejecting an impossible value (negative density) computed during the first step. The danger of this approach is that the solution could have diverged to such an unrealistic condition when negative density occurs that recovery is very difficult.

Section 3
CONCLUSIONS

The following conclusions were reached as a result of this analysis:

1. Closed form analytical methods and spatial marching numerical techniques are inadequate for treating base recirculation flows with regions of subsonic flow; however, either time-dependent or relaxation finite difference numerical techniques may be used to analyze these flows.

2. Techniques are not currently available for locating and treating shock waves as discrete discontinuities between finite difference grid points; therefore, shock smearing techniques using pseudo viscosity must be used.

3. It appeared neither practical nor necessary to include viscous terms in this analysis.

4. A recent version of a two-step Lax-Wendroff time-dependent, finite-difference technique appeared to be the most attractive numerical scheme for solving the three-dimensional base recirculation flow field.

5. A cylindrical coordinate system greatly simplified the application of boundary conditions.

6. Stretching transformations are desirable to concentrate grid points near regions where the flow is complicated by shock waves of plume interactions.

7. A rapid access drum storage routine of the Univac 1108 digital computer provides an acceptable alternative to the limiting core storage of this computer.

8. It is possible to solve for the total energy of the flow at each grid point as a function of the local density and velocity components. This constitutes using a steady-state form of the energy equation and permits reduction of storage variables by 20%.

9. Computation time can be significantly reduced by beginning with an initial flow field from a single nozzle calculated by the method of characteristics.

10. Because of the complexity of the flow field, it is not possible to mathematically calculate the largest possible time step which will yield a stable solution. An alternative technique is suggested by which the maximum stable time step is estimated as slightly less than that given by the CFL condition. Stability is then monitored either by comparing changes of flow variables or checking for negative density.

Section 4
RECOMMENDATIONS

Although the objective of this investigation was to develop a technique for predicting the base recirculation flow field of Saturn-class launch vehicles, the method appears applicable for Space Shuttle configurations. It is, therefore, recommended that modifications to this technique be explored so that base recirculation of Space Shuttle vehicles may be computed.

In principle, the numerical technique described in Section 2.4 of this report should be capable of predicting a base recirculation flow field with shock waves occurring as smeared shocks over several grid points. However, such a vast number of grid points might be required to adequately define the shock wave patterns that this technique could be wholly unattractive from a computational standpoint. It is also questionable if the amount of mass reversed by a detached smeared shock near a reflection plane or centerline will adequately approximate the mass reversed by a true detached shock which will be infinitesimally thin. For these reasons it is recommended that some future effort be directed toward improving numerical methods so that shock waves could be located between grid points and treated as discrete discontinuities. Independent Research efforts at Lockheed/Huntsville into such areas as finite-element applications to fluid mechanics could provide an attractive alternative technique for the solution of such complex three-dimensional flow fields.

A literature survey also indicated that there exists a lack of quantitative information as to what happens in the region of plume impingement and resulting shock detachment. Such essential information as the dominating parameters controlling the shock detachment height and magnitudes of reversed flow components behind a strong shock are still unknown. This problem is akin to blunt body flow, and it is believed that much could be learned about dominant terms and controlling parameters as has recently been done for blunt bodies by Brainerd and Waldrop (Ref. 10).

Section 5
REFERENCES

1. Brewer, Edwin B., and Charles E. Craven, "Experimental Investigation of Base Flow Field at High Altitude for a Four-Engine Clustered Nozzle Configuration," NASA TN D-5164, May 1969.

2. Whitehurst, Charles A., and Jeffrye Mourer, "Jet-Shock Interactions," J. Astronautical Sci., Vol. V, No. 11, March-April 1968, pp. 71-79.

3. D'Attorre, L., G. Nowak, and H. U. Thommen, "Inviscid Analysis of the Plume Created by Multiple Rocket Engines," General Dynamics/Convair Report GD/C-DBE-66-014, May 1966.

4. Prozan, Robert J., and Douglas E. Kooker, "The Error Minimization Technique with Application to a Transonic Nozzle Solution," J. Fluid Mech., to be published.

5. Von Neumann, J., and R. D. Richtmyer, "A Method for the Numerical Calculation of Hydrodynamic Shocks," J. Appl. Phys., Vol. 21, No. 3, March 1950, pp. 232-237.

6. Lax, P. D., and B. Wendroff, "Systems of Conservation Laws," Comm. Pure Appl. Math., Vol. 13, No. 2, May 1960, pp. 217-237.

7. MacCormack, Robert W., "The Effect of Viscosity in Hypervelocity Impact Cratering," AIAA Paper No. 69-354, May 1969.

8. Moretti, Gino, "Importance of Boundary Conditions in the Numerical Treatment of Hyperbolic Equations," Proceedings of the International Symposium on High-Speed Computing in Fluid Dynamics, Phys. Fluids, Vol. 12, No. 12, December 1969.

9. D'Attorre, L., Private Communication, November 1969.

10. Brainerd, J. J., and W. R. Waldrop, "The Plasma Sheath in the Nose Region of Selected Reentry Bodies," UARI Research Report No. 60, September 1968.